

Superparamagnetic particle dynamics and mixing in a rotating capillary tube with a stationary magnetic field

Jun-Tae Lee · Aamir Abid · Ka Ho Cheung ·
L. Sudheendra · Ian M. Kennedy

Received: 3 January 2012 / Accepted: 1 April 2012 / Published online: 18 April 2012
© Springer-Verlag 2012

Abstract The dynamics of superparamagnetic particles subject to competing magnetic and viscous drag forces have been examined with a uniform, stationary, external magnetic field. In this approach, competing drag and magnetic forces were created in a fluid suspension of superparamagnetic particles that was confined in a capillary tube; competing viscous drag and magnetic forces were established by rotating the tube. A critical Mason number was determined for conditions under which the rotation of the capillary prevents the formation of chains from individual particles. The statistics of chain length was investigated by image analysis while varying parameters such as the rotation speed and the viscosity of the liquid. The measurements showed that the rate of particle chain formation was decreased with increased viscosity and rotation speed; the particle dynamics could be quantified by the same dimensionless Mason number that has been demonstrated for rotating magnetic fields. The potential for enhancement of mixing in a bioassay was assessed using a fast chemical reaction that was diffusion-limited. Reducing the Mason number below the critical value, so that chains were formed in the fluid, gave rise to a modest improvement in the time to completion of the reaction.

Keywords Magnetic particles · Particle chains · Rotating capillary · Mason number

1 Introduction

Microfluidics has popularized the study of biomolecular interactions in small volumes due to faster assay times, reduced reagent consumption, integrated multiple assay steps, portability, and cost effectiveness (Ganguly et al. 2010; Zhou et al. 2010; Herr et al. 2007). Microfluidic flow is usually dominated by laminar flow in a low-Reynolds number regime and the interaction between reagents in the fluid is limited to diffusion, which is time consuming as large molecules (organic and biological) with very low diffusivities are involved in the biomolecular interactions. The strategies to improve interactions between biomolecules can be categorized into passive and active mixing methods. Passive methods are based on the perturbation of fluids caused by its flow through a maze of geometrical structures (Johnson et al. 2002; Chandrasekaran and Packirisamy 2008). Active methods are aided by external forces to generate chaotic advection to increase the interfacial area. Examples include electrokinetic driving forces to mix electrolytic fluids (Fu et al. 2005); non-contact magnetic force-controlled superparamagnetic nanoparticle manipulation (Kim and Park 2005); manipulation of microliter sized droplets using ferrofluids dynamics (Song et al. 2007); piezoelectric transducers (PZT) to create ultrasonic vibration (Liu et al. 2003), and hydrodynamic interaction; and alternating electroosmotic flows such as micropumps (Kim et al. 2009a; Derks et al. 2008).

Recent studies have shown that the manipulation of magnetic particles has promise as a platform for fast mixing, as complex magnetic fields and flows are easily generated (Derks et al. 2007). In addition, magnetic particles can be synthesized with custom properties such as high surface to volume ratio for bio-molecular binding, chemical functionality to improve binding of biomolecules and

J.-T. Lee · A. Abid · K. H. Cheung · L. Sudheendra ·
I. M. Kennedy (✉)
Department of Mechanical and Aerospace Engineering,
University of California Davis, One Shields Avenue,
Davis, CA 95616, USA
e-mail: imkenney@ucdavis.edu

can be applied in homogeneous assays that avoid additional washing steps. Frank et al. (2009) demonstrated enhanced mixing of superparamagnetic particles in small liquid volumes under a rotating magnetic field with a change of particle chain length that correlated with changes in relative velocities. Linked chains of magnetic particles have been used in a rotating magnetic field to mix fluids in microchannels with increasingly chaotic fluid trajectories (Biswal and Gast 2004a); chains of magnetic particles were shown to be active micro-stirrers to achieve enhanced mixing (Kang et al. 2007); and dynamic actuation of superparamagnetic particles has been shown to enhance microfluidic perfusion (Moser et al. 2009).

For maximum probability of interaction between a reaction site on the surface of a magnetic particle and the analyte in solution, agglomeration should be avoided when the liquids are subjected to magnetic fields. Agglomeration (random 3D assembly) reduces the analyte–antibody interaction probability due to inaccessibility of the analyte to the core of the agglomerate. Having magnetic particles assemble as chains (an organized 1D assembly) increases the interaction probability and eases the transport within microfluidic devices. This enhanced interaction between magnetic particle-bound antibodies and the analyte is further improved by applying competing forces—magnetic forces and viscous drag. Sensitive biosensors require a satisfactory balance between moderate magnetic fields that move particles within fluids and enhance mixing, without the tendency for particles to aggregate and diminish the effective surface area and the number of binding sites.

Previous studies on magnetic particle mixing were based on the superparamagnetic particles in rotating magnetic fields that were created by the phased excitation of a quadrupole arrangement of electromagnets. These systems can present several challenges such as undesirable heat generation by the electromagnets and limited optical access. Unintentional heating results in undetermined and uncontrolled effects in systems that involve chemical and biological reactions. Furthermore, the quadrupole electromagnet is not an ideal arrangement for a small scale, low power, and portable biosensor. This paper presents a new design for fluid mixing based on an active mixing approach, employing superparamagnetic particles with magnetic and viscous counter forces. To overcome some of the challenges of a rotating magnetic field, we propose the inverse, i.e., a rotating capillary tube in a fixed magnetic field, to achieve the same result. The rotating capillary establishes a forced or rotational vortex in which there is no fluid shear and the motion can be described as a solid body rotation. In addition, there is no radial velocity. This simple motion provides an accurately known velocity field at low particle concentrations, in which the magnitude of the fluid velocity increases linearly with distance from the axis. The use of capillaries

has various advantages. Adaptors and feed-through standards for capillary systems have been developed for gas and high-pressure chromatography technology. Many companies sell small rotary unions to couple rotating and stationary parts. This makes the use of capillaries appealing in a simple, off-the-shelf device. Capillaries also provide options for liquid-core light guiding, making it a versatile option for both absorption and fluorescence detection.

The formation of chains of magnetic particles in a fluid has been examined in the context of ferrofluids and the impact on the rheological properties of the mixtures (Thurm and Odenbach 2003; Ghasemi et al. 2008). Ferrofluids are used in magnetic bearings, as seals on shafts, as a heat transfer medium in loudspeakers, among other examples. The formation of chains affects the viscosity of the suspension. In this study, we experimentally examine the formation of chains in a micro-capillary system with combined optical microscopy and image analysis. A measure of the enhancement of mixing was obtained using the mixing-limited reaction between HRP (Horseradish peroxidase) enzymes and a colorless substrate in a colorimetric assay.

2 Experiment

A borosilicate capillary tube (Friedrich & Dimmock, NJ), outside radius = 600 μm , inside radius (r_c) = 450 μm was used in all the experiments. The capillary tube was attached to an electrically controlled motor (Tamiya, Japan). The DC motor was used to control the rotation speed as shown in Fig. 1. The initial condition for all experiments consisted of uniformly dispersed single particles; the magnetic field and rotation of capillary tube were applied simultaneously at $t = 0$. The magnetic field was applied for at least 25 min to investigate the steady-state rate of particle chain formation at different angular velocities.

Two permanent rectangular (50.8 mm long, 12.7 mm wide and 3.17 mm thick) Neodymium-Iron-Boron magnets (Magcraft, VA) were symmetrically placed on either side of the capillary tube, such that the axis perpendicular to the largest area of the magnet and the corresponding magnetic field was perpendicular to the axis of the capillary tube (Fig. 2). The strength of the magnetic field was controlled by changing the distance between the two magnets; the maximum magnetic field of 300 mT was measured with a Gauss meter (Transcat, NY). The uniformity of the magnetic field was confirmed both experimentally and numerically (Vizimag 3.19), avoiding magnetic gradients that would lead to deposition of particles onto the inner wall of the tube.

The superparamagnetic particles were purchased from Bangslabs, Inc. (5 % solids by weight, Fishers, IN). Superparamagnetic magnetite nanoparticles (7.1 wt%) are dispersed in a micron sized polymer bead. The mean

Fig. 1 Schematic illustration of the experimental setup and optical images of magnetic particle chains under a stationary magnetic field inside the capillary tube from top. ($B = 10$ mT, magnetic particle diameter, $d_p = 2.85$ μm , 0.06 wt% solids; $\omega = 0.49$ rad/s)

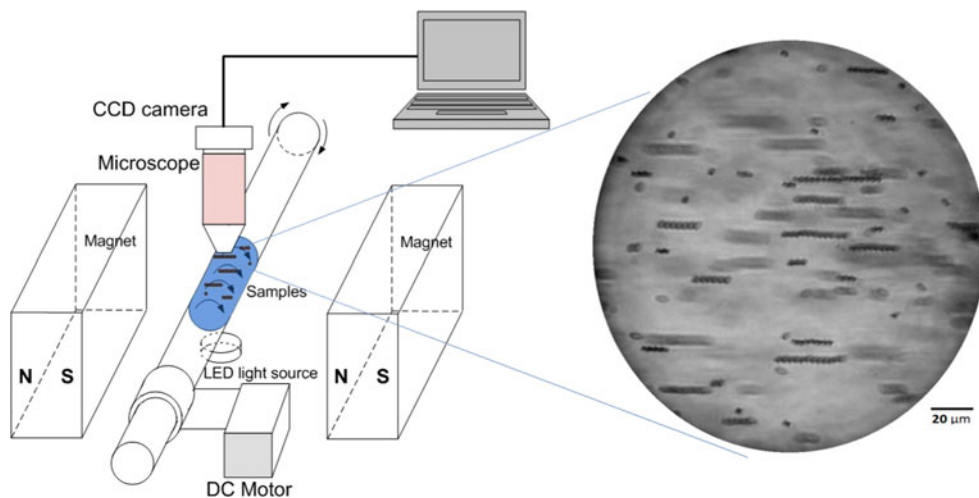
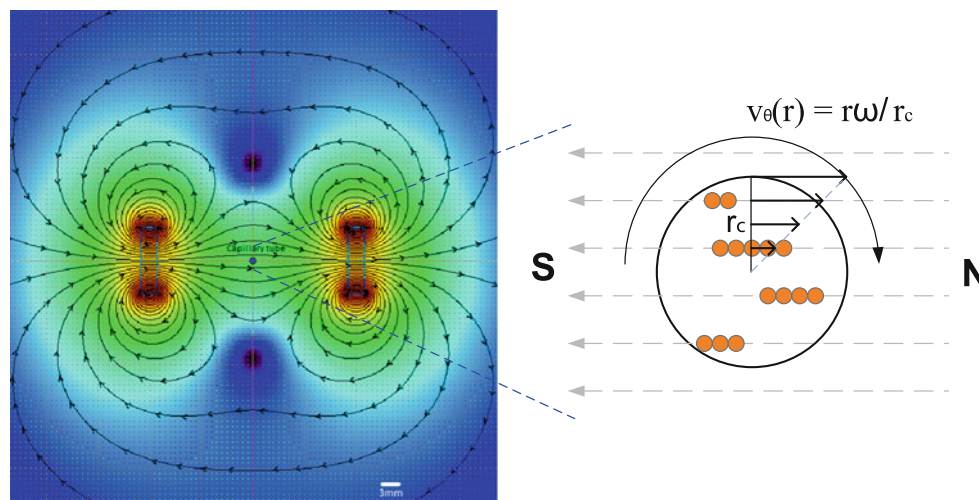


Fig. 2 Magnetic fields were simulated with Vizimag software (Vizimag[®] 3.193). Neodymium-Iron-Boron permanent magnets with 12.7 mm height and 3.17 mm width from Magcraft, VA were located 37 mm apart. The capillary is at the center of the magnets. A blow-up schematic of the capillary is shown to the right. The radius of the capillary is r_c and r is the coordinate distance from the axis of the capillary



particle diameter was $d = 2.85$ μm , density $\rho = 1,230$ kg/m^3 , and the particle susceptibility $\chi = 0.597$. The measured particle susceptibility captures the demagnetizing field formed by the particle. The particles were diluted to 0.06 wt% solids in 1 mM PBS (Phosphate buffered saline) solution; a volume of 1 μL of suspension was used in all experiments. In addition, the capillary tube was rinsed with PEG (Polyethylene glycol) solution to prevent adhesion of the particles onto the inner wall of the tube. Glycerol was added in all cases to the buffer solution to change the viscosity of the liquid. The viscosities of glycerol–water mixtures for different mass concentrations are shown in Table 1. The viscous drag force experienced

by the particles was adjusted by either varying the rotational speeds ω of the capillary tube and or by adjusting the fluid viscosity with the addition of glycerol to water. In addition, glycerol was used to adjust the refractive index for improved particle image resolution. The capillary tube was subjected to steady rotation with angular velocities ω which varied from 0.05 to 0.817 rad s^{-1} . The particles were freely suspended in the buffer solution in the absence of magnetic field, but when the magnetic field was applied, they began forming chains.

To visualize the particles, an in-house imaging system was built. It consisted of an objective lens (50 \times , Mitutoyo, Japan), binocular microscope system (Sciencescope, NC),

Table 1 Water–glycerol viscosities

	10 % glycerol	30 % glycerol	40 % glycerol
Temperature (22 °C)	$\eta = 1.314 \times 10^{-3}$ Pa s	$\eta = 2.820 \times 10^{-3}$ Pa s	$\eta = 4.497 \times 10^{-3}$ Pa s

and CCD camera (Tucsen imaging technology, China). A time interval of 142 ms and resolution of $2,580 \times 1,944$ pixels were used to take particle images during rotation of the tube (Fig. 1). The depth of focus was about 25 μm . Particle imaging in the capillary was limited to a region close to the capillary wall as a result of excessive scattering from particles at locations distant from the wall. The poor quality of the images at more central locations in the capillary prohibited the collection of data at these locations. As a result, particles that were more than 50 μm from the inner wall of the capillary were not considered for image analysis due to the poor resolution of the particles. The images of particle chains were recorded on a computer from the CCD camera and processed using image analysis software (ImageJ, NIH). Images of chains are shown in Fig. 1.

Superparamagnetic particles coated with horseradish peroxidase (HRP) enzyme and a buffer solution containing the chromogenic substrate tetramethylbenzidine (TMB) were used to investigate the mixing rate between the solution and the magnetic particles. HRP was conjugated to the magnetic particles following a standard protocol (Kim et al. 2009b). Particles were suspended in 1 ml of dried DMF and *N*-hydroxysulfosuccinimide (sulfo-NHS, 0.06 mmol) and 1-[3-(dimethylamino)propyl]-3-ethylcarbodiimide hydrochloride (EDC, 0.05 mmol); the mixture were incubated overnight at room temperature in a rotating mill. After a single wash, the particles were extracted by a magnetic. HRP solution was added to the particles and the mixture was shaken for 4 h at room temperature. The HRP-conjugated magnetic particles were suspended with PBS. HRP substrate buffer was prepared by adding 400 μl of 0.6 % TMB in dimethyl sulfoxide (DMSO) and 100 μl of 1 % hydrogen peroxide (H_2O_2) into 25 ml of citrate-acetate buffer. A white light-emitting diode (LED) was used to measure the change in the optical density of the liquid; the absorbance was a measure of reaction at the particle surface and was used as a measure of mixing. The absorbance of the liquid was followed for 20–30 min by Photodiode (FDS010, Thorlabs, NJ) for different Mason numbers.

3 Results and discussion

The characteristics of the magnetic particles, such as chain length and the abundance of chains, depend on the strength of the magnetic field and its gradients, the magnetization of the particles, the viscosity of the medium, and in our case the rotational speed of the capillary; these quantities can be expressed in terms of a non-dimensional group, the Mason number. The Mason number, Mn , is defined as the ratio of a hydrodynamic force to the magnetic interaction force. Several studies have used the dimensionless Mason number

to describe the particle dynamics induced by a rotating magnetic field with different proportionality factors (Kang et al. 2007; Krishnamurthy et al. 2008); in this study we define Mn in a similar manner to Biswal and Gast (2004a) as

$$Mn = \frac{32\eta\omega}{\mu_0\chi^2H_0^2}, \quad (1)$$

where η is the viscosity of the fluid, ω is the angular velocity of the capillary tube, μ_0 is the magnetic permeability of vacuum, χ is the particle susceptibility, and H_0 is the external magnetic field strength. For large Mn , viscous drag forces dominate magnetic forces and cause the chains, formed under the influence of the magnetic field, to break-up (Melle and Martin 2003). Mason numbers between 0.92×10^{-3} and 15.1×10^{-3} were applied in our experiments by changing the parameters affecting the drag force and viscosity. Variation of the Mason number permitted examination of the influence of the key parameters on the rate of particle chain formation. We have studied the relative velocity of both single particles and chains relative to the suspending fluid. The single particles offer a convenient measure of the fluid velocity in the absence of an external magnetic field, given the fact that they closely follow the steady, low-Reynolds number flow in the capillary. The single-particle Stokes number (St) was calculated to be 2.54×10^{-5} ; for a $St \ll 1$, the particles follow the fluid velocity.

Three distinct effects are at play in the dynamics of superparamagnetic particles in a rotating flow field: self-assembly of single particles into chains due to the induced magnetic moment of particles; torque on the rotating chains by the external magnetic field; and viscous drag of the fluid due to chain rotation relative to the fluid. In the case of a rotating magnetic field and stationary fluid, chains rotate about an axis at the same frequency as the magnetic field with a retarded phase angle (Melle et al. 2000). For the case of a rotating capillary with a fixed uniform magnetic field, chains follow the fluid that rotates as a solid body with the magnetic moment vector of the chains pointed in the direction of the magnetic field.

Video microscopy imaging was used to quantify chain growth at varying Mason numbers. In Fig. 3, the rate of particle chain formation is shown for different rotational speeds. The average length of a chain was determined from 70 individual measurements of chain length that was defined as the number of single particles that were members of the chain. Average chain length $L(t)$ was calculated based on the number of particles.

$$L(t) = \frac{\sum n_i}{N}, \quad (2)$$

where n_i = number of particles per chain and N = total number of chains.

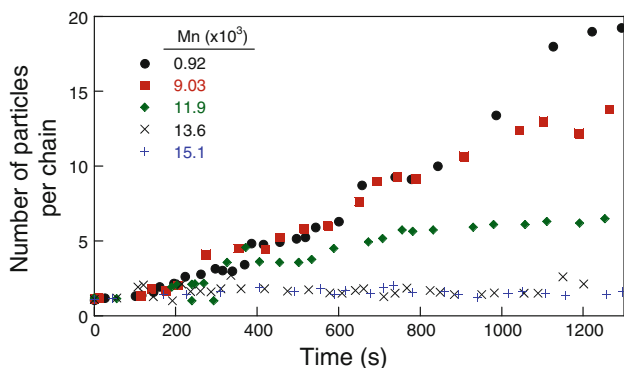


Fig. 3 Average number of particles per chain with different angular velocities in a constant external magnetic field (0.06 wt% solids, 10 mT, 30 % glycerol)

For a given ω or Mason number, chain length increased with time for $Mn < 0.012$. For $Mn \geq 0.012$ no chain formation was observed, suggesting a critical Mason number above which the fluid drag forces dominate the interparticle magnetic attractive forces. The growth of chains as a function of time was also observed for particles in a stationary fluid (Promislow et al. 1995) and particles in shear flow (Brunet et al. 2005). Based on Smoluchowski’s kinetic equation, Promislow et al. (1995) applied a scaling argument to describe chain growth where mean chain length $\langle S(t) \rangle \sim t^z$. They showed that when the drag force is proportional to the chain size (where chain diffusivity is inversely proportional to chain size), $z = 0.5$. Their experimental results typically gave z values between 0.45 and 0.75 for varying particle concentrations and magnetic fields which indicated enhanced particle diffusivities for higher z values. Similar scaling analysis of our data shows comparable results as seen in Fig. 4. The data are obtained from experiments with $Mn < 0.012$, where chain growth is observed. The power law fit to the data indicates that $z = 0.84$, suggesting strong enhancement of particle chain formation over a broad range of Mn . This enhancement can

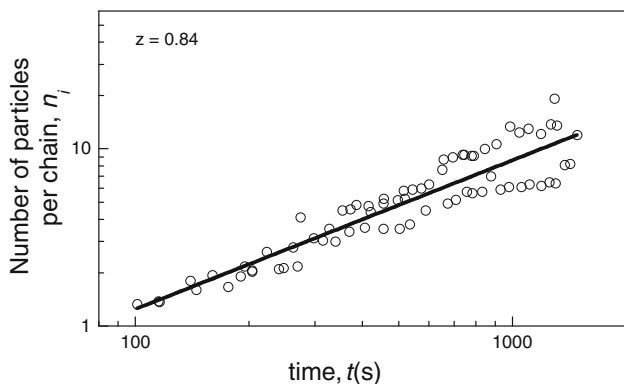


Fig. 4 Number of particles per chain as a function of time re-plotted for scaling. Data are from experiments where $Mn < 0.012$

be attributed to the large dimensionless dipole strength λ (ratio of magnetic energy to thermal energy) where $\lambda = (\pi\mu_0 d^3 M^2)/(72k_B T)$ with μ_0 the magnetic permeability in a vacuum, d the bead diameter, M the bead magnetization, k_B the Boltzmann constant, and T the temperature of the fluid. The dipole strength calculated for the magnetic particles is 4500, over two orders of magnitude larger than that studied by Promislow et al. (1995). This enhanced magnetic attraction can result in rigid chains with high local fields, leading to enhanced chain growth rates and the persistence of linear chains against fluid drag. The motion of chains, relative to the fluid that contains unbound single particles, leads to single particle scavenging by rotating chains and an enhanced growth rate beyond that found in quiescent conditions.

To gauge the impact of rotation on chain growth and on mixing in a capillary under a uniform external magnetic field, we need to understand the relative motion of the particle chains with respect to the fluid. Figure 5 presents a cartoon of the motion of rigid chains in a rotating capillary with a solid body rotation, both with and without a uniform external magnetic field. In the absence of a magnetic field, a cross (in this case represented as two imaginary orthogonal particle chains) will move with the fluid without deforming. To a fixed observer, the cross appears to rotate but there is no rotation or motion relative to the fluid—and hence no mixing. When the magnetic field is present, a chain will attempt to rotate to follow the fluid motion, but will be torqued by the magnetic field to align along the magnetic field lines. To execute each realignment, the chain must undergo a 90° counter-clockwise rotation with respect to the fluid for each 90° clockwise rotation of the capillary, sweeping through a quadrant of the fluid. A full 360° rotation of the capillary leads to a corresponding 360° counter rotation of the chains. In effect, each chain behaves as a small rotor, sweeping through the fluid. The picture is similar to the observations of Kang et al. (2007). The images of chains in our capillary indicate that there is a sufficient population of chains of sufficient length that much of the fluid in the capillary will be interrogated by rotating chains (Fig. 1).

The images of the single particle and chains were used to estimate velocities. Figure 6 shows snapshots of time-lapse images of single particles and a chain. The single particles move at a velocity that is very close to the expected velocity of the fluid, as determined by a solid body rotation. However, the chain moves at a slightly slower speed; the velocity difference between the fluid and chains ranged 5–10 $\mu\text{m/s}$; this difference is greater than the measurement error that results from the depth of focus $f \sim 25 \mu\text{m}$ of the imaging system (resulting in an estimated velocity uncertainty of $\sim 4.4 \mu\text{m/s}$ due to radial

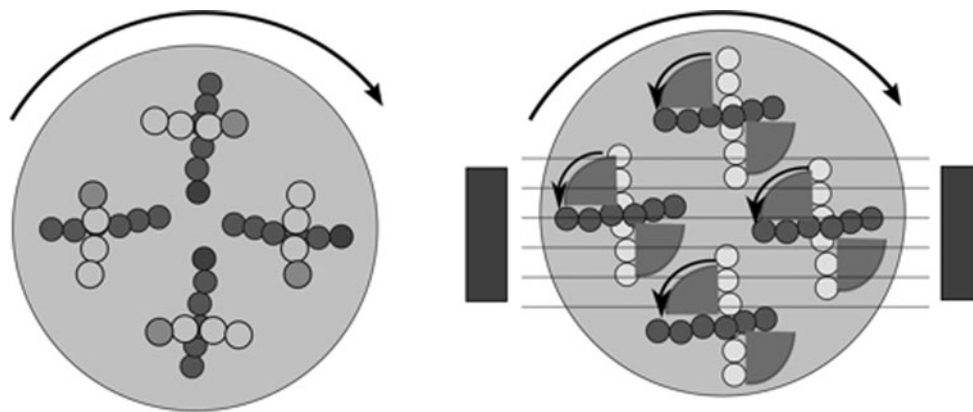


Fig. 5 Illustration of chain motion in a rotating capillary. On the *left*, no magnetic field. A cross of chains rotates with the solid body motion of the fluid without deformation. On the *right*, a magnetic field causes the chains to continuously re-align with the magnetic field. The realignment is shown at four locations. At each location, the *light*

gray chains indicate the position of the chain if it had simply followed a solid body rotation from the previous quadrant. The chain rotates 90° between each quadrant to achieve realignment with the external field. A segment of fluid is swept out by the chain as it realigns with the field

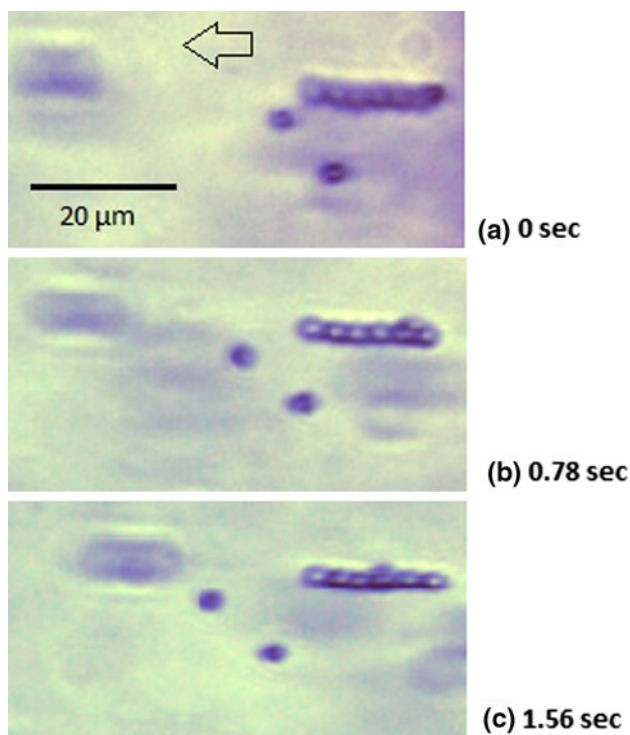


Fig. 6 Images of single particle and particle chains. *Arrow* indicates the direction of the rotating capillary tube. ($B = 10$ mT, 0.06 wt% solids, 10 % glycerol, $\omega = 0.176$ rad/s). **a** 0 s, **b** 0.78 s, **c** 1.56 s

position uncertainty). Biswal and Gast (2004b) showed that it was possible for the motion of chains to become asynchronous with the rotation of their external magnetic field above a certain Mason number.

The impact of the rotation of chains on mixing and biochemical reaction was examined directly using HRP enzyme-coated magnetic particles and colorless TMB

substrate. This reaction set was chosen because it provided a system that was diffusion-limited rather than kinetically limited. The relative rates of diffusion versus chemical reaction are characterized by the Damkohler number, Da ; a large Damkohler number indicates that the chemical reaction is limited by diffusion or mixing. The rate constant for the reaction of TMB with HRP is $k = 3.6 \times 10^6 \text{ M}^{-1}\text{s}^{-1}$; the diffusion coefficient of TMB in water is $3.1 \times 10^{-10} \text{ m}^2\text{s}^{-1}$ (Marquez and Dunford 1997; Baldrich et al. 2009). For our conditions, the Damkohler number was above 4×10^6 . Hence, this reaction pair provides a suitable measure of mixing and diffusion. We found that the progress of the reaction between the two reactants (HRP and TMB) was improved when the magnetic field was applied across the rotating capillary (Fig. 7). The presence of magnetic field (at our lowest Mason number condition at which chains are formed) reduced the time for quasi-completion of reaction by about a factor of two.

It must be noted that an optimum Mason number for mixing has not been determined in this study. Clearly sub-critical Mason numbers are required to form chains that are needed for enhanced mixing. Too small a Mason number will lead to undesirable aggregation. An operationally optimum Mason number for optimum mixing rates should exist. In practice, the magnetic field should be stronger than the field used in this work. One would expect that chains will form more quickly in a stronger magnetic field and so the assay time will be reduced. An increase of the field strength requires a concomitant increase in the rotational speed to achieve a critical Mason number. The higher rotational speeds required under stronger field conditions prevented successful imaging of the faster moving particles and chains in our set-up. Therefore, all the results here have been obtained under the conditions of constant magnetic

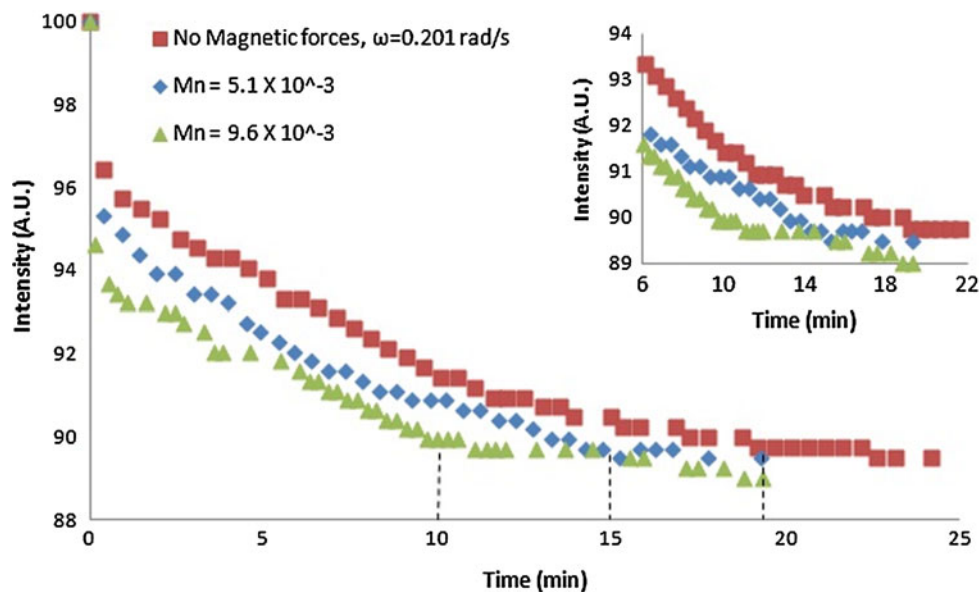


Fig. 7 Percentage transmittance of the TMB substrate as a function of time. HRP enzymes that catalyze the TMB substrate were coated on magnetic particles that were introduced into the capillary along with buffer medium containing TMB substrate. The color of the solution changed as reaction of the TMB proceeded, causing the transmissivity of light to be reduced as a result of absorbance.

field strength for which imaging was feasible. However, we expect that under actual conditions of a bioassay, when particle imaging is not a concern, a stronger field and faster rotational speed will improve the speed of the assay considerably compared to the conditions pertaining in the current study.

4 Conclusion

Superparamagnetic particle dynamics were evaluated in a rotating flow field in a capillary tube by studying the average chain length. The particles in the capillary tube formed chains and lined up along the magnetic field. The Mason number was changed by changing the rotational speed of the capillary and the viscosity of the suspending fluid. Magnetic particle chain length increased linearly with time for Mason numbers smaller than 0.012. Our results showed the presence of a critical Mason number for the inhibition of chain growth from single particles. When chains are created, their rotational motion relative to the fluid can enhance mixing and the progress of biochemical reactions. A kinetically fast reaction was used to assess mixing. Reducing the Mason number so that chains formed was found to enhance the progress of the HRP-TMB reaction. An ideal Mason number for an actual bioassay would promote chain formation and relative motion of the chains without the formation of aggregates that lose surface

The curves show the mixing of the solution for different Mason numbers. In all cases, the experiments started at a normalized intensity of 100. Dashed lines indicate the approximate times when the reactions reached completion. The inset focuses on the results at around 10 min of mixing time (0.06 wt% solids, 4.24 mT, 10 % glycerol)

area and reaction sites. A practical application of the principles set forth here would involve a stronger magnetic field and faster rotational speed of the capillary to enhance the speed of an assay.

Acknowledgments The project described was supported by Award Number P42ES004699 from the National Institute of Environmental Health Sciences. The content is solely the responsibility of the authors and does not necessarily represent the official views of the National Institute of Environmental Health Sciences or the National Institutes of Health. This work was also supported by Grant 200911634 from NIAID, NIH and by USDA Grant Number 2009-35603-05070. The assistance of Jon Nellis in building the optical system is greatly appreciated.

References

- Baldrich E, del Campo FJ, Munoz FX (2009) Biosensing at disk microelectrode arrays. Inter-electrode functionalisation allows formatting into miniaturised sensing platforms of enhanced sensitivity. *Biosens Bioelectron* 25(4):920–926
- Biswal SL, Gast AP (2004a) Micromixing with linked chains of paramagnetic particles. *Anal Chem* 76(21):6448–6455
- Biswal SL, Gast AP (2004b) Rotational dynamics of semiflexible paramagnetic particle chains. *Phys Rev E* 69(4)
- Brunet E, Degre G, Okkels F, Tabeling P (2005) Aggregation of paramagnetic particles in the presence of a hydrodynamic shear. *J Colloid Interface Sci* 282(1):58–68
- Chandrasekaran A, Packirisamy M (2008) Enhanced bio-molecular interactions through recirculating microflows. *NanoBiotechnology* 2(2):39–46. doi:10.1049/iet-nbt:20070029

- Derks RJS, Dietzel A, Wimberger-Friedl R, Prins MWJ (2007) Magnetic bead manipulation in a sub-microliter fluid volume applicable for biosensing. *Microfluid Nanofluid* 3(2):141–149
- Derks RJS, Frijns AJH, Prins MWJ, Dietzel AH (2008) Self-organized twinning of actuated particles for microfluidic pumping. *Appl Phys Lett* 92(2)
- Franke T, Schmid L, Weitz DA, Wixforth A (2009) Magneto-mechanical mixing and manipulation of picoliter volumes in vesicles. *Lab Chip* 9(19):2831–2835
- Fu LM, Yang RJ, Lin CH, Chien YS (2005) Novel microfluidic mixer utilizing electrokinetic driving forces under low switching frequency. *Electrophoresis* 26(9):1814–1824. doi:10.1002/elps.200410222
- Ganguly R, Hahn T, Hardt S (2010) Magnetophoretic mixing for in situ immunochemical binding on magnetic beads in a microfluidic channel. *Microfluid Nanofluid* 8(6):739–753
- Ghasemi E, Mirhabibi A, Edrissi M (2008) Synthesis and rheological properties of an iron oxide ferrofluid. *J Magn Magn Mater* 320(21):2635–2639
- Herr AE, Hatch AV, Throckmorton DJ, Tran HM, Brennan JS, Giannobile WV, Singh AK (2007) Microfluidic immunoassays as rapid saliva-based clinical diagnostics. *Proc Nat Acad Sci USA* 104(13):5268–5273. doi:10.1073/pnas.0607254104
- Johnson TJ, Ross D, Locascio LE (2002) Rapid microfluidic mixing. *Anal Chem* 74(1):45–51. doi:10.1021/Ac010895d
- Kang TG, Hulsen MA, Anderson PD, den Toonder JMJ, Meijer HEH (2007) Chaotic mixing induced by a magnetic chain in a rotating magnetic field. *Phys Rev E* 76(6):066303 (066301–066311)
- Kim KS, Park JK (2005) Magnetic force-based multiplexed immunoassay using superparamagnetic nanoparticles in microfluidic channel. *Lab Chip* 5(6):657–664
- Kim B, Yoon S, Lee K, Sung H (2009a) Development of a microfluidic device for simultaneous mixing and pumping. *Exp Fluids* 46(1):85–95
- Kim HJ, Ahn KC, Gonzalez-Techera A, Gonzalez-Sapienza GG, Gee SJ, Hammock BD (2009b) Magnetic bead-based phase anti-immunocomplex assay (PHAIA) for the detection of the urinary biomarker 3-phenoxybenzoic acid to assess human exposure to pyrethroid insecticides. *Anal Biochem* 386(1):45–52
- Krishnamurthy S, Yadav A, Phelan PE, Calhoun R, Vuppu AK, Garcia AA, Hayes MA (2008) Dynamics of rotating paramagnetic particle chains simulated by particle dynamics, Stokesian dynamics and lattice Boltzmann methods. *Microfluid Nanofluid* 5(1):33–41
- Liu RH, Lenigk R, Druyor-Sanchez RL, Yang JN, Grodzinski P (2003) Hybridization enhancement using cavitation microstreaming. *Anal Chem* 75(8):1911–1917
- Marquez LA, Dunford HB (1997) Mechanism of the oxidation of 3,5,3',5'-tetramethylbenzidine by myeloperoxidase determined by transient- and steady-state kinetics. *Biochemistry* 36(31):9349–9355
- Melle S, Martin JE (2003) Chain model of a magnetorheological suspension in a rotating field. *J Chem Phys* 118(21):9875–9881
- Melle S, Fuller GG, Rubio MA (2000) Structure and dynamics of magnetorheological fluids in rotating magnetic fields. *Phys Rev E* 61(4):4111–4117
- Moser Y, Lehnert T, Gijs MAM (2009) Quadrupolar magnetic actuation of superparamagnetic particles for enhanced microfluidic perfusion. *Appl Phys Lett* 94(2):022505 (022501–022503)
- Promislow JHE, Gast AP, Fermigier M (1995) Aggregation kinetics of paramagnetic colloidal particles. *J Chem Phys* 102(13):5492–5498
- Song WB, Ding ZW, Son C, Ziaie B (2007) Aqueous microdrop manipulation and mixing using ferrofluid dynamics. *Appl Phys Lett* 90(9)
- Thurm S, Odenbach S (2003) Particle size distribution as key parameter for the flow behavior of ferrofluids. *Phys Fluids* 15(6):1658–1664
- Zhou Y, Wang Y, Lin QA (2010) A microfluidic device for continuous-flow magnetically controlled capture and isolation of microparticles. *J Microelectromech Syst* 19(4):743–751